Semnan University

Progress in Physics of Applied Materials

journal homepage: https://ppam.semnan.ac.ir/

Ni-Doped Cu10%/YIG Nanoparticle-Based Metamaterials: Synthesis and Electromagnetic Property Investigation at Terahertz Frequencies

Fatemeh Delkhosh [a], Ali Bahari [a*], Reza Gholipur [b]

[a] *Department of Solid-State Physics, University of Mazandaran, Babolsar, 4741695447, Iran*

[b] *Department of Physics, Faculty of Science, Razi University, Kermanshah, Iran*

ARTICLE INFO

Article history:
Received: 11 November 2024
Revised: 12 December 2024
Accepted: 12 December 2024

Keywords:
Metamaterials;
Terahertz Materials;
Double-Negative (DNG) Materials;
Cu10%/YIG Composites;
Nickel-Doped Nanoparticles;
Refractive Index.

ABSTRACT

In this study, we examine the negative electromagnetic properties and refractive index in yttrium iron garnet (*YIG*) -based nanocomposites, specifically *Cu10%/YIG* and nickel-doped *Cu10%/YIG*, synthesized via an in-situ method. Field Emission Scanning Electron Microscopy (FESEM) analysis confirmed the successful formation of the target nanostructures. Particle size distribution analysis indicated an approximately normal and uniform distribution across the *YIG* nanoparticles. UV spectroscopy verified that the electronic structure and optical properties of the samples matched predicted characteristics Measurements of dielectric permittivity and magnetic permeability were conducted at room temperature using scattering parameters from a Vector Network Analyzer (VNA) and processed through MATLAB software. The results showed simultaneous negativity in both ε and μ within certain frequency ranges, confirming the potential for a negative refractive index.This feature opens promising opportunities for advanced electromagnetic wave control, with implications for optical, communication, and electronic technologies.

1. Introduction

Metamaterials, an emerging domain within materials science and physics, first garnered attention in the late 1960s [1], with significant advances following in the 1990s and early 2000s [2, 3]. Initial theoretical work by Victor Veselago in 1967 proposed the concept of materials with negative refractive indices and unusual electromagnetic behaviors [1]. For many years, these ideas remained largely theoretical due to fabrication limitations. However, by the early 2000s, researchers succeeded in creating the first functional metamaterials with engineered structures and tailored electromagnetic properties. Early pioneers such as David Smith and John Pendry catalyzed the field's rapid expansion, setting the stage for its wide-ranging applications in optics, telecommunications, and nanotechnology [3].

The unique properties of metamaterials are determined primarily by their designed structure. Unlike natural materials, metamaterials can exhibit extraordinary optical and electromagnetic characteristics. Among their notable features are a negative refractive index [4], phase inversion [5], and the ability to focus electromagnetic fields [6]. These properties make metamaterials suitable for advanced applications, including super - lensing [7], cloaking [8], high-resolution imaging systems [9], and controlled light and electromagnetic wave scattering [10], thereby positioning them at the forefront of modern technological innovation.

The refractive index, a fundamental property dictating how light bends as it passes through a material, can be negative in metamaterials, particularly at specific wavelengths. This negative refractive index makes it possible for new optical effects to happen, like reverse lensing effects and better imaging technologies. Doping and compositing techniques can also improve the properties of metamaterials, making them more useful for advanced optical and device uses [11].

* Corresponding author. Tel.: +98-911-2537702
E-mail address: a.bahari@umz.ac.ir

Cite this article as:
Delkhosh F., Bahari A., and Gholipur R., 2024. Ni-Doped Cu10%/YIG Nanoparticle-Based Metamaterials: Synthesis and Electromagnetic Property Investigation at Terahertz Frequencies. *Progress in Physics of Applied Materials*, *5*(1), pp.31-38. DOI: **10.22075/PPAM.2024.35886.1122**
© 2025 The Author(s). Progress in Physics of Applied Materials published by Semnan University Press. This is an open-access article under the CC-BY 4.0 license. (https://creativecommons.org/licenses/by/4.0/)

The electromagnetic parameters of a material, specifically dielectric permittivity (ε) and magnetic permeability (μ), are critical in defining its response to an applied electromagnetic wave [12, 13]. Based on these parameters, metamaterials can be categorized into four main types. The first type includes materials where both ε and μ are positive, characteristic of typical transparent dielectrics. The second type consists of materials with positive magnetic permeability but negative dielectric permittivity, often found in electrical plasmas and known as "single-negative metamaterials." The third type, referred to as negative-index or "left-handed" materials, includes those with both ε and μ negative, commonly labeled as "double-negative metamaterials." The fourth category comprises materials with negative magnetic permeability and positive dielectric permittivity, also known as "magnetic plasmas." These last three categories fall under the classification of metamaterials, utilizing artificial micro- and nanostructures to achieve their distinct properties [14, 15]. Some effects of these materials, like the Doppler [16] and Cherenkov effects [17], make them behave in ways that are very different from normal materials. Metamaterials are further classified by application into microwave, terahertz, and photonic metamaterials.

A defining feature of metamaterials is the potential for negative permittivity and permeability, which has substantial implications in optics and supports advanced and novel optical functionalities.

S-parameters, specifically S_{11} and S_{21}, are vital in characterizing the electromagnetic response of metamaterials. The S_{11} parameter represents the reflection coefficient of an incoming wave at a surface, while S_{21} describes the transmission coefficient between two points. These parameters are directly related to the permittivity and permeability of metamaterials, providing a foundation for their design and optimization across applications [18]. Their unique characteristics allow precise control of electromagnetic waves in the terahertz frequency range, enabling pioneering applications in imaging, sensing, and wireless communications. The tunability and subwavelength features of metamaterials enhance device performance, driving technological innovation. Current research focuses on advanced fabrication techniques and material combinations. Integrating metamaterials with nanostructures shows significant potential by enhancing nonlinear optical properties and enabling precise light control, promising breakthroughs in high-resolution imaging and sensor sensitivity. Additionally, combining metamaterials with composite materials can improve mechanical properties and flexibility, with transformative possibilities for wearable technology and flexible electronics. These structures can also be engineered to respond at specific frequencies, enabling tailored applications in telecommunications, biomedical devices, and environmental monitoring [19].

Yttrium Iron Garnet (*YIG*) is a particularly noteworthy material in materials science and electronics, recognized since the 1950s for its unique electromagnetic properties and valued in radiofrequency and microwave applications. Known as a low-loss dielectric with high magnetic resonance, *YIG* functions as a nonlinear magnetic medium in various electronic devices [20]. Its magnetic properties derive from its crystal structure, composed of iron and yttrium atoms, allowing for tunability and doping with elements such as gallium and lutetium [21, 22]. Doping YIG can modify its electrical and magnetic properties, enhancing its performance in targeted applications. Metamaterials gain their distinct characteristics primarily from their structure, and controlling this structure and composition can significantly enhance their electromagnetic response. Among various composites, metal-based composites have drawn particular attention.

In this study, an in-situ method was used to make a 10 wt% Cu10%/YIG nanocomposite with nickel doping. This was done to get negative electromagnetic parameters and a negative refractive index. Measurements were performed within the 5-8 THz frequency range. The S_{11} and S_{21} parameters were recorded using an HP 8510 Network Analyzer, and the ε and μ parameters were subsequently extracted through MATLAB software.

2. Experimental

In this study, we synthesized the nanocomposite $Ni_{0.001}/Cu10\%/YIG$ by combining specific ratios of precursor powders. Initially, stoichiometric quantities of Y_2O_3 and Fe_2O_3were mixed in a 5:3 molar ratio and annealed at 600°C for six hours, yielding $Y_3Fe_5O_{12}$ (YIG) nanocomposites via an in-situ synthesis process. Following this, 10 wt% of CuO powder was added to the YIG to form the Cu10%/YIG compound, and subsequently, 0.001 g of NiO nanopowder was incorporated into the Cu10%/YIG mixture.

The synthesized compositions—YIG, Cu10%/YIG, and $Ni_{0.001}/Cu10\%/YIG$—were each dispersed in pure ethanol and subjected to ball milling for 10 hours. Following milling, the samples were centrifuged and dried in a vacuum oven at 80°C. The resulting dried powders were then sieved through a 320-mesh screen. Each powder was pressed into $22.8 \times 10.1 \times 3\ mm^3$ rectangular bars under 30 MPa pressure and sintered at 1050°C for one hour. To complete the synthesis process, these compacted bars were placed in a tube furnace filled with 99.9% pure hydrogen gas at 500°C for three hours. The resulting bars were prepared for subsequent experimental analysis.

To examine the negative permittivity (ε) and permeability (μ) properties of the synthesized nanocomposites, the scattering parameters the S_{11} and S_{21}were measured. Each rectangular sample was carefully positioned in a fixture to ensure thorough interaction with the incident electromagnetic waves. The fixture containing the sample was connected to the ports of a Vector Network Analyzer (VNA). Electromagnetic waves were transmitted from the VNA's input port, passed through the sample, and exited at the output port, with the analyzer recording the reflected S_{11} and transmitted S_{21} signals. These measurements were conducted over the 5–8 THz frequency range. The metamaterial properties of the nanocomposites were validated by calculating the permittivity and permeability values based on the scattering parameters, using MATLAB software. The refractive index was also derived from these values.

Field Emission Scanning Electron Microscopy (FESEM) was used to analyze the nanoscale structures and surface

characteristics of the synthesized materials. As a high-resolution imaging technique, FESEM provides detailed visualizations of the sample surfaces. Fig. 1 presents the FESEM images of the *YIG*, *Cu10%/YIG*, and $Ni_{0.001}/Cu10\%/YIG$ samples annealed at 600°C. Using ImageJ software, we calculated the average particle size for each sample. Histogram fitting revealed a log-normal particle size distribution, as depicted in Fig. 2.

The FESEM images and particle size distribution graphs in Figs. 1 and 2 demonstrate that the addition of copper and nickel nanoparticles to *YIG* significantly enhances both particle size and distribution. The original *YIG* sample exhibits a structure with larger, more agglomerated particles, with an average particle size of 57.94 nm. With the addition of 10 wt% copper to *YIG*, the average particle size decreases to 36.50 nm, and the particle distribution becomes more uniform.

This reduction in size and improvement in particle dispersion can be attributed to the catalytic effects and structural stabilization provided by copper, which in turn enhances the nanocomposite's optical and magnetic properties.

Subsequently, the introduction of a small amount of nickel of Cu10%/YIG further reduces the average particle size to 21.57 nm and results in an even more uniform particle distribution. This additional reduction in size and increase in active surface area arise from the synergistic effects of nickel and copper, leading to enhanced plasmonic and magnetic properties in the nanocomposite. Overall, the combination of Ni and Cu with *YIG* yields nanocomposites with optimized particle size and improved dispersion, characteristics that are highly valuable for advanced photonic and magnetic applications.

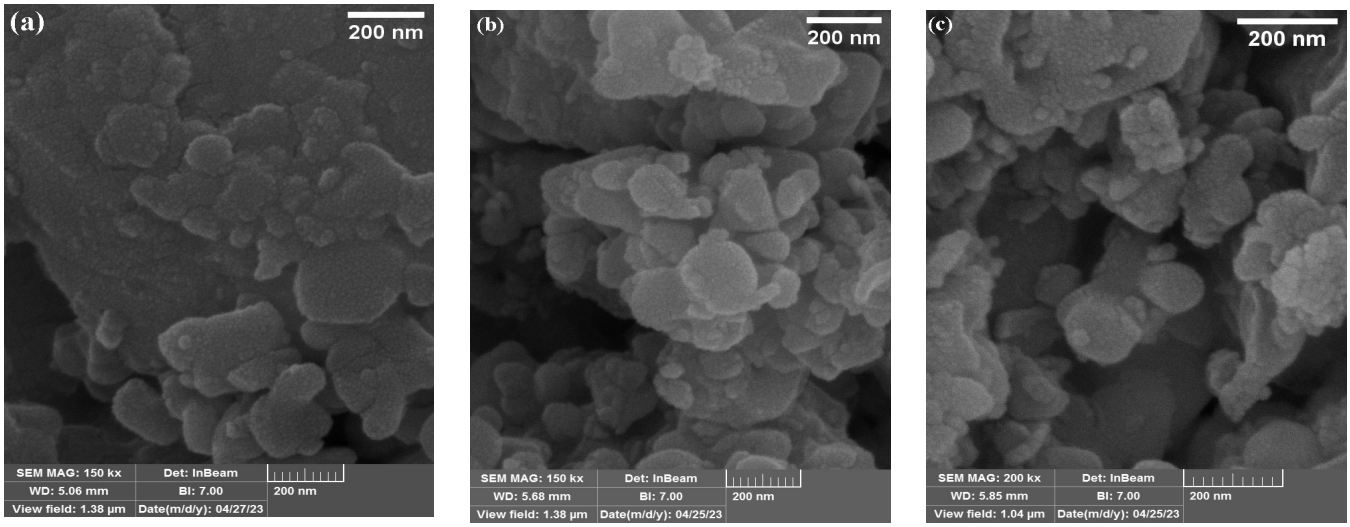

Fig. 1. FESEM images of *YIG*, *Cu10%/YIG*, and $Ni_{0.001}/Cu10\%/YIG$ samples

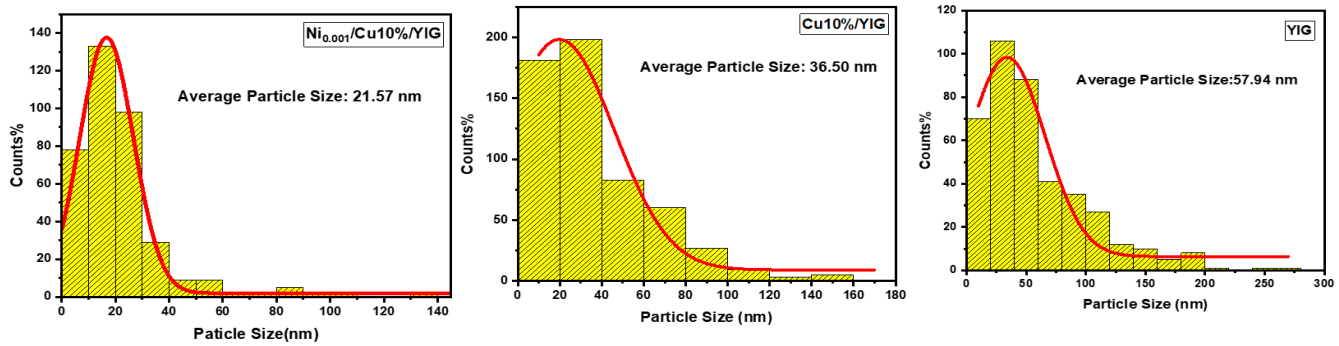

Fig. 2. Grain size distribution histogram of average particle size for *YIG*, Cu10%/YIG, and $Ni_{0.001}$/Cu10%/YIG samples

Ultraviolet (UV) analysis was performed to investigate the optical and electromagnetic characteristics of the samples, providing insight into their light absorption and transmission behaviors. This analysis aids in the development of materials with unique optical properties. Absorption peaks in the UV spectrum for *YIG* and copper- and nickel-doped compositions were identified within the wavelength range of 190–1000 nm, as illustrated in Fig. 3.

The results indicate that the Ni sample exhibits the highest absorption, particularly in the ultraviolet region, attributed to plasmonic interactions induced by the presence of nickel nanoparticles. *YIG*, lacking metallic nanoparticles, demonstrates lower absorption with relatively smoother absorption curves. This difference in absorption behavior highlights the impact of surface plasmon effects and the increased density of electronic states in the presence of nickel nanoparticles, enhancing the metamaterial optical properties of these nanocomposites.

The addition of copper to *YIG* results in increased absorption in both the visible and ultraviolet regions, forming the *Cu10%/YIG* structure, which displays

heightened absorption due to the plasmonic properties of copper. Introducing nickel to *Cu10%/YIG* creates a synergistic interaction between nickel and copper nanoparticles, leading to further enhanced absorption, especially in the ultraviolet range. This $Ni_{0.001}/Cu10\%/YIG$ combination, with its strong absorption and improved optical properties, presents an ideal candidate for advanced photonic and optical applications.

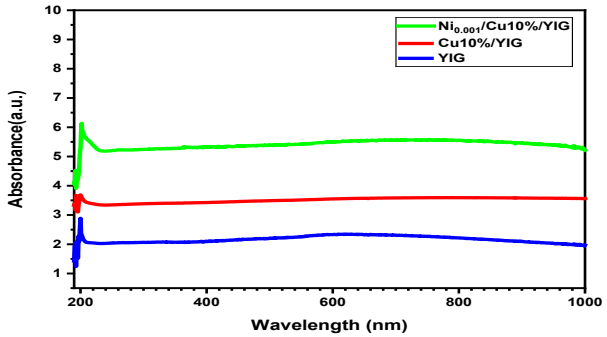

Fig. 3. UV spectra of *YIG, Cu10%/YIG, and* $Ni_{0.001}/Cu10\%/YIG$ samples

S-parameters, specifically S_{11} and S_{21}, are fundamental metrics for assessing device performance in microwave and RF engineering, including applications in metamaterials. The parameter S_{11}, known as the input reflection coefficient, quantifies the portion of power reflected back to the input upon signal application. A low S_{11} value indicates efficient power transfer and optimal impedance matching, both of which are crucial for the effective functioning of metamaterials. In contrast, S_{21} represents the forward transmission coefficient, measuring the power transferred from the input to the output of the device .

Simultaneous analysis of S_{11} and S_{21} provides valuable insights into energy propagation and scattering characteristics within metamaterials, informing the design and optimization of devices such as cloaking mechanisms, superlenses, and advanced sensors, where precise control over wave interactions is essential. By minimizing S_{11} and maximizing S_{21}, researchers can enhance metamaterial performance, paving the way for innovative electromagnetic applications [23].

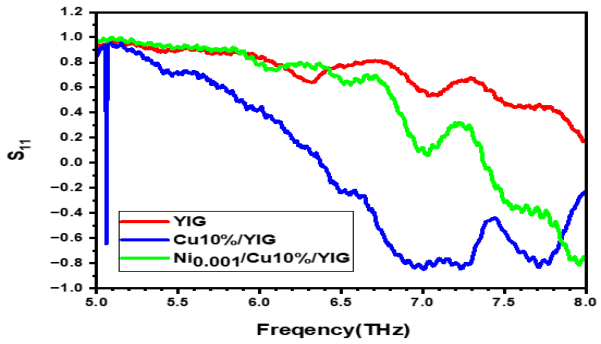

Fig. 4. S_{11} Parameter

As shown in Fig. 4, the scattering parameter $S_{11}$was analyzed over the frequency range of 5 to 8 THz for three metamaterial nanocomposite samples: *YIG, Cu10%/YIG*, and $Ni_{0.001}/Cu10\%/YIG$. The results indicate that the *YIG* sample exhibits high reflection due to strong magnetic resonance, with S_{11} values remaining close to 1 across much of the frequency range. The addition of copper in the *Cu10%/YIG* sample reduces reflection, and S_{11}reaches negative values at certain frequencies, indicating a phase reversal of the reflected wave. These changes arise from partial energy absorption by copper and spin interactions at the *YIG* surface.

Introducing a small amount of nickel into the *Cu10%/YIG* structure further decreases the intensity of S_{11}. The presence of nickel enhances magnetic damping and increases wave energy absorption, reducing the overall reflection of the sample. This behavior suggests a more complex interaction between the layers and highlights the effect of nickel and copper on magnetic damping and reflection. Negative S_{11} values at certain frequencies indicate ferromagnetic-like behavior and demonstrate the potential of these nanocomposites for applications in wave absorbers, frequency filters, and terahertz sensors.

In Fig. 5, the scattering parameter S_{21} for three metamaterial nanocomposites—*YIG*, *Cu10%/YIG*, and$Ni_{0.001}/Cu10\%/YIG$—is examined over the frequency range of 5 to 8 THz. The S_{21} plot, representing the power transmitted through the samples, displays pronounced oscillations and peaks due to magnetic and electromagnetic resonances within this frequency range. The *YIG* sample, due to its inherent magnetic properties, exhibits lower S_{21} values, indicating higher energy absorption. With the addition of copper to *YIG*, the *Cu10%/YIG* sample shows increased S_{21} values, which can be attributed to copper's conductivity and the reduction of magnetic reflection.

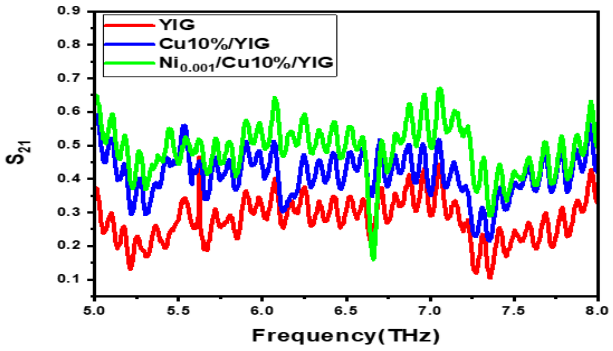

Fig. 5.S_{21}Parameter of *YIG, Cu10%/YIG, and* $Ni_{0.001}/Cu10\%/YIG$ samples

In the $Ni_{0.001}/Cu10\%/YIG$ sample, the inclusion of a small amount of nickel in *Cu10%/YIG* further enhances power transmission at certain frequencies, with S_{21} values surpassing those of the *Cu10%/YIG* sample. These changes are due to the presence of nickel and the more complex spin interactions between layers, which improve wave transmission and reduce reflection. Overall, the addition of copper and nickel to *YIG* improves wave transmission properties and generates distinct frequency oscillations, making these composites suitable for applications such as terahertz filters and absorbers.

In Fig. 6, the real part of the permittivity ε' for the three materials *YIG, Cu10%/YIG*, and $Ni_{0.001}/Cu10\%/YIG$ is compared across the frequency range of 5 to 8 THz. The *YIG* plot exhibits a relatively stable, fluctuation-free response, indicating the material's consistent dielectric response to

electromagnetic fields within this frequency range. However, with the addition of copper to *YIG*, the ε' values show significant oscillations, with large peaks especially evident at frequencies above 6.5 THz. These changes are attributed to surface plasmon resonances induced by the nanoscale structure and metamaterial properties of *Cu10%/YIG*, leading to stronger interactions with the electromagnetic field.

The introduction of a small amount of nickel into *Cu10%/YIG* further intensifies the oscillations, producing more pronounced resonant peaks at frequencies above 7 THz. This increase in oscillations and the appearance of sharper peaks indicate that the presence of nickel enhances the frequency dispersion and the material's anomalous response to electromagnetic waves. Overall, adding copper and then nickel to *YIG* results in an increasingly anomalous dielectric behavior, characterized by greater oscillations, resonant peaks, and negative ε' values in certain frequency ranges due to plasmonic resonances and the complex nanocomposite structure.

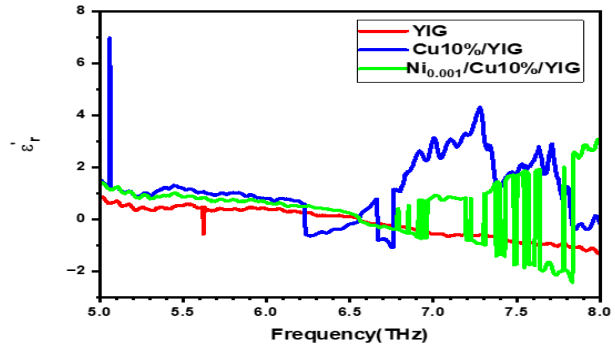

Fig. 6. Real part of the dielectric permittivity as a function of frequency in the 5–8 THz range

In Fig. 7, the imaginary part of the permittivity, ε'', is analyzed for three materials—*YIG*, *Cu10%/YIG*, and $Ni_{0.001}/Cu10\%/YIG$—over the frequency range of 5 to 8 terahertz. The results indicate that pure *YIG* displays low and relatively stable fluctuations, reflecting a weak response to electromagnetic waves in this frequency range. When copper is added to *YIG*, significant oscillations and a decrease in ε'' values toward negative numbers are observed, indicating the occurrence of resonance phenomena due to the metamaterial structure of *Cu10%/YIG*.

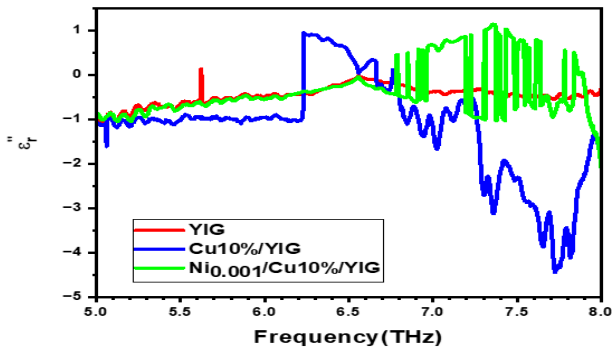

Fig. 7. Imaginary part of the dielectric permittivity as a function frequency in the 5–8 THz range

Adding a small amount of nickel to *Cu10%/YIG* further increases the oscillations and produces stronger peaks at certain frequencies. These changes suggest that the presence of nickel enhances negative feedback and creates more allowed and forbidden frequency regions, which appear as sharp peaks on the graph. Overall, adding metals like copper and nickel to YIG makes surface plasmonic effects stronger and spreads out frequencies more evenly in these metamaterials. This makes them behave in strange ways as dielectrics and have negative ε values at some frequencies.

In Fig. 8, the behavior of the real part of the relative permeability $\mu'$for the three materials—*YIG*, *Cu10%/YIG*, and $Ni_{0.001}/Cu10\%/YIG$—is analyzed over the frequency range of 5 to 8 terahertz. The results show that pure *YIG* exhibits stable and nearly constant behavior, but a sharp peak appears at 6.5 terahertz, indicating the occurrence of *YIG*'s natural magnetic resonance. This peak results from the ferromagnetic response of *YIG* to magnetic fields within this frequency range and reflects the effect of magnetic resonance on the sudden increase in μ'.

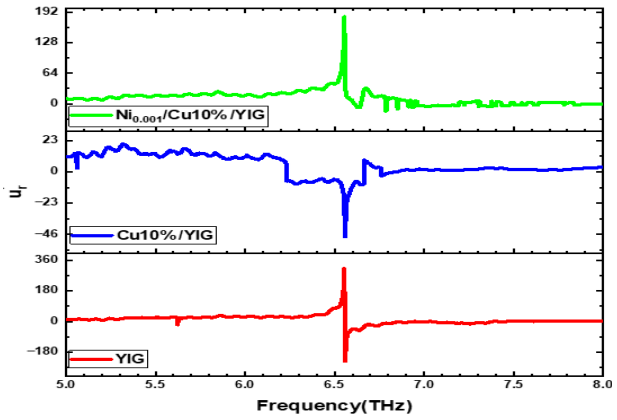

Fig. 8. Real part of magnetic permeability as a function of frequency in the 5–8 THz range

Adding copper to *YIG* induces oscillations in μ' with both positive and negative values, which indicate plasmonic resonance phenomena and reflective characteristics within the nanocomposite structure. When a small amount of nickel is added to *Cu10%/YIG*, these oscillations and peak values become more intense, especially at frequencies above 6.5 terahertz. These changes are due to the formation of stronger magnetic resonances and larger peaks, resulting from complex interactions between nickel and the metamaterial structure of the nanocomposite. Overall, the sequential addition of copper and nickel to *YIG* enhances its unusual magnetic properties and increases the occurrence of negative values and resonant peaks, which may be advantageous for high-frequency applications and tuning the electromagnetic properties of materials.

In Fig. 9, the imaginary part of the relative permeability μ'' for three nanocomposite metamaterial samples—*YIG*, *Cu10%/YIG*, and $Ni_{0.001}/Cu10\%/YIG$—is examined over the frequency range of 5 to 8 terahertz. The results indicate that *YIG* exhibits a strong peak around 6.5 terahertz, which is attributed to spin resonance associated with its

metamaterial structure. When copper is added to *YIG*, the intensity of this peak decreases, suggesting a weakening of magnetic resonance due to changes in spin boundary conditions. Additionally, the inclusion of a small amount of nickel in $Ni_{0.001}/Cu10\%/YIG$ further reduces the peak intensity, which is attributed to spin interactions between nickel and *YIG*.

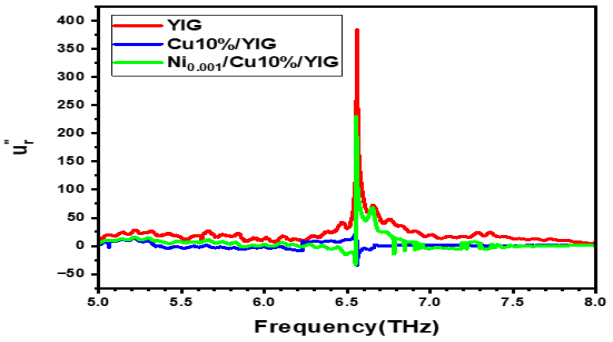

Fig. 9. Imaginary part of magnetic permeability as a function of frequency in the 5–8 THz range

This gradual reduction in peak intensity with the addition of copper and nickel indicates a decrease in magnetic oscillations and a reduced influence of spin resonance. Moreover, the observation of negative permeability values at certain frequencies reflects ferromagnetic behavior in these nanocomposites, likely due to unusual magnetic responses at the nanoscale. These properties, particularly in $Ni_{0.001}/Cu10\%/YIG$, highlight potential applications in the design of frequency absorbers, advanced filters, and magnetic sensors.

The refractive index n of a material, defined as the ratio between the speed of light in a vacuum and its speed within that material, can be represented by the following equation [24]:

$$n = \frac{c}{v} = \sqrt{\varepsilon\mu} \tag{1}$$

where c is the speed of light in a vacuum (approximately $3 \times 10^8 \frac{m}{s}$), and v is the speed of light within the material. The refractive index encapsulates the interaction between light and the material, influencing properties such as the degree of light bending (refraction) and light absorption. Typically, the refractive index consists of both real and imaginary components:

$$n = n' + in'' \tag{2}$$

In this expression, n' represents the material's refractive behavior, such as light bending, while n'' denotes optical losses, quantifying the extent of light absorption as it travels through the material.

For standard materials, n' generally has positive values, with larger values indicating increased light refraction. Meanwhile, n'', typically positive and relatively small, reflects minor light absorption where some light energy converts to heat. However, in metamaterials, both $n'$and n'' can vary significantly across different frequencies, potentially resulting in a negative refractive index. This phenomenon arises from the unique structural properties and particle arrangements in metamaterials, enabling them to exhibit behaviors not found in conventional materials. Such a refractive index not only characterizes the optical behavior of metamaterials but also reveals distinctive properties that offer groundbreaking possibilities in optics and photonics. Therefore, while the refractive index in ordinary materials provides insight into standard light-matter interactions, enabling conventional optical applications, metamaterials present unprecedented potential for advanced control of light.

The refractive index n can be derived from the real and imaginary parts of both the dielectric permittivity and magnetic permeability, as expressed by the following equations [24]:

$$\varepsilon = \varepsilon' + i\varepsilon'' \tag{3}$$

$$\mu = \mu' + i\mu'' \tag{4}$$

These equations link the refractive index to the fundamental electromagnetic properties of the material, providing a comprehensive framework for analyzing and engineering optical properties.

The expressions for $n'$and n'' can be obtained by substituting equations (2), (3), and (4) into equation (1). These expressions are as follows:

$$n' = \sqrt{\frac{(\varepsilon'\mu' - \varepsilon''\mu'') + \sqrt{(\varepsilon'\mu'' + \varepsilon''\mu')^2 + (\varepsilon'\mu' - \varepsilon''\mu'')^2}}{2}} \tag{5}$$

$$n'' = \frac{(\varepsilon'\mu'' + \varepsilon''\mu')\sqrt{\frac{(\varepsilon'\mu' - \varepsilon''\mu'') + \sqrt{(\varepsilon'\mu'' + \varepsilon''\mu')^2 + (\varepsilon'\mu' - \varepsilon''\mu'')^2}}{2}}}{(\varepsilon'\mu' - \varepsilon''\mu'') + \sqrt{(\varepsilon'\mu'' + \varepsilon''\mu')^2 + (\varepsilon'\mu' - \varepsilon''\mu'')^2}} \tag{6}$$

In these equations, $n'$and $n''$are the real and imaginary parts of the refractive index, respectively. Equation (5) defines n' based on the real and imaginary components of the permittivity ε' and ε'' and permeability μ' and μ'', representing the material's refractive properties. Similarly, equation (6) defines n'', which characterizes the optical losses, quantifying the material's absorption of light.

These relationships highlight how both the real and imaginary parts of the refractive index are influenced by the intrinsic electromagnetic properties of the material,

providing valuable insights into its optical behavior.

As shown in Fig. 10, the real part of the refractive index as a function of frequency (5 to 8 THz) has been analyzed for *YIG*, *Cu10%/YIG*, and $Ni_{0.001}/Cu10\%/YIG$. All three samples exhibit a decrease in the refractive index with increasing frequency, yet they display sharp peaks at certain frequencies. These peaks are likely due to surface plasmon resonances or magneto-electric resonances stemming from the nanoscale structure and the metamaterial properties of the materials. The sample containing nickel, in particular, shows more pronounced fluctuations and sharper peaks at higher frequencies, which may be attributed to stronger resonances induced by nickel.

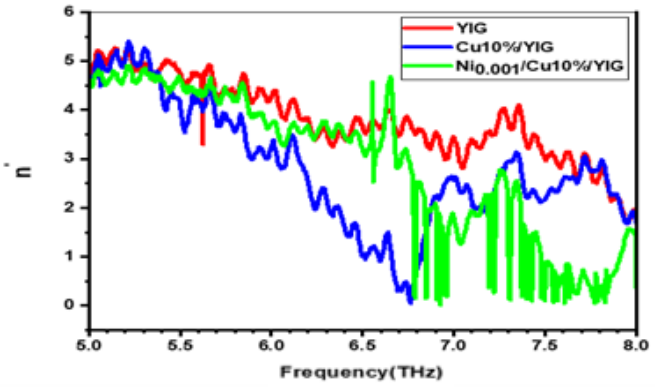

Fig. 10. Real refractive index as a function of frequency

Adding copper to *YIG* leads to an increase in the refractive index and enhances plasmonic resonances in the lower frequency range, as copper is a strong conductor and amplifies surface plasmonic effects. In contrast, incorporating nickel into the *Cu10%/YIG* composite produces additional peaks, especially at higher frequencies; nickel possesses unique magnetic properties that intensify magnetic resonances, resulting in greater fluctuations in the real part of the refractive index. These findings suggest that the addition of copper and nickel to *YIG* enhances the optical and magnetic properties of the metamaterial across different frequency ranges.

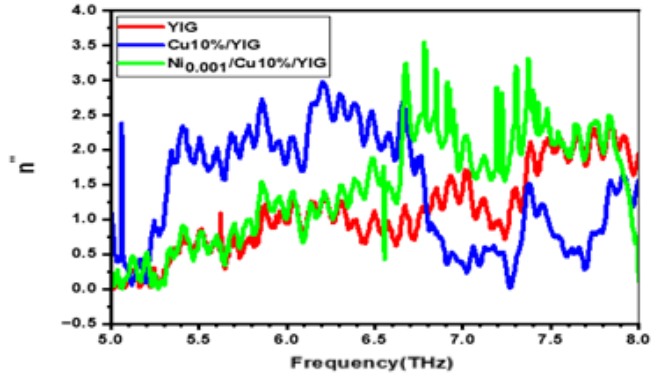

Fig. 11. Imaginary refractive index as a function of frequency

The imaginary part of the refractive index in the frequency range of 5 to 8 THz, shown in Fig. 11, displays multiple peaks in electromagnetic energy absorption. These peaks are attributed to surface plasmon and magnetic resonances arising from the nanoscale structure of these materials. Each sample, due to its unique composition, shows maximum energy absorption at different frequencies. For example, the sample containing nickel exhibits sharper peaks at higher frequencies, which can be attributed to the magnetic properties of nickel. Negative values at certain points in the chart indicate a unique metamaterial behavior, where instead of absorbing, the material acts as a wave amplifier, potentially enhancing energy at these frequencies.

The addition of copper to *YIG* increases energy absorption at lower frequencies due to plasmon resonances introduced by copper. When nickel is also incorporated into the *Cu10%/YIG* composition, additional peaks, especially at higher frequencies, emerge, indicating enhanced magnetic resonances. Thus, the *Cu10%/YIG* composite with nickel improves the metamaterial's electromagnetic absorption and transmission properties over a wider frequency range, making it valuable in designing metamaterial structures with greater control over optical and magnetic properties.

3. Conclusions

In this study, *YIG*, *Cu10%/YIG*, and $Ni_{0.001}/Cu10\%/YIG$ nanocomposites were successfully synthesized using an in-situ method at 600°C. The substitution of iron with copper and nickel in the *YIG* structure was demonstrated to be feasible, as evidenced by FESEM images that clearly illustrated these substitutions. The chemical composition, functional groups, and chemical bonds were confirmed using UV spectroscopy. In the terahertz frequency range (5-8 THz), S-parameters were measured with a VNA, and the dielectric permittivity ε and magnetic permeability μ values were calculated using MATLAB.

Analysis of both the real and imaginary components of dielectric permittivity and magnetic permeability revealed intricate relationships between the nanoscale structure and optical properties. The results underscore that the optical characteristics of the materials, such as the refractive index, are directly influenced by variations in permittivity and permeability, suggesting the potential for double-negative (DNG) behavior. This dependency enhances our understanding of optical phenomena such as light absorption, scattering, and magnetic resonances. Overall, this study not only looks into the materials' magnetic and electrical properties, but it also shows how important it is for these properties to be related to how they behave optically. This paves the way for the creation of new materials in optical and nanoelectronics technologies.

To optimize the performance of DNG materials, this study explored various concentrations of copper and nickel, with the detailed results to be presented in future work. This research enables a precise assessment of how changes in the concentrations of these elements affect the magnetic and electrical properties of DNG materials.

Conflicts of interest

The authors declare that they have no known competing financial interests or personal relationships that could have appeared to influence the work reported in this paper.

Authors contribution statement

Conceptualization; Data curation; Formal analysis; Investigation; Methodology; Project administration; Resources; Software; Supervision; Validation; Visualization; Roles/Writing – original draft; Writing – review & editing.

Fatemeh Delkhosh: Investigation, data collection, synthesis, analysis, conceptualization, methodology development, resource management, writing, drafting the original manuscript, and editing.

Ali Bahari: Project management, supervision, acquisition of funding, validation, manuscript review, and editing.

Reza Gholipur: Supervision, manuscript review and editing, validation.

References

[1] Veselago, V.G., 1967. The electrodynamics of substances with simultaneously negative values of and. *Usp. fiz. nauk*, *92*(3), pp.517-526.

[2] Takagi, T., 1990. A concept of intelligent materials. *Journal of Intelligent Material Systems and Structures*, *1*(2), pp.149-156.

[3] Smith, D.R., Padilla, W.J., Vier, D.C., Nemat-Nasser, S.C. and Schultz, S., 2000. Composite medium with simultaneously negative permeability and permittivity. *Physical review letters*, *84*(18), p.4184.

[4] Smith, D.R., Padilla, W.J., Vier, D.C., Nemat-Nasser, S.C. and Schultz, S., 2000. Composite medium with simultaneously negative permeability and permittivity. *Physical review letters*, *84*(18), p.4184.

[5] Chen, H.T., Padilla, W.J., Cich, M.J., Azad, A.K., Averitt, R.D. and Taylor, A.J., 2009. A metamaterial solid-state terahertz phase modulator. *Nature photonics*, *3*(3), pp.148-151.

[6] Veselago, V.G., 2003. Electrodynamics of materials with negative index of refraction. In *Electromagnetic Materials* (pp. 115-122).

[7] Fang, N. and Zhang, X., 2002, August. Imaging properties of a metamaterial superlens. In *Proceedings of the 2nd IEEE Conference on Nanotechnology* (pp. 225-228). IEEE.

[8] Schurig, D., Mock, J.J., Justice, B.J., Cummer, S.A., Pendry, J.B., Starr, A.F. and Smith, D.R., 2006. Metamaterial electromagnetic cloak at microwave frequencies. *Science*, *314*(5801), pp.977-980.

[9] Wood, B., Pendry, J.B. and Tsai, D.P., 2006. Directed subwavelength imaging using a layered metal-dielectric system. *Physical Review B—Condensed Matter and Materials Physics*, *74*(11), p.115116.

[10] Xie, P., Shi, Z., Feng, M., Sun, K., Liu, Y., Yan, K., Liu, C., Moussa, T.A., Huang, M., Meng, S. and Liang, G., 2022. Recent advances inradio-frequency negative dielectric metamaterials by designing heterogeneous composites. *Advanced Composites and Hybrid Materials*, *5*(2), pp.679-695.

[11] Shalaev, V.M., 2007. Optical negative-index metamaterials. *Nature photonics*, *1*(1), pp.41-48.

[12] Wang, N., Tong, J., Zhou, W., Jiang, W., Li, J., Dong, X. and Hu, S., 2015. Novel quadruple-band microwave metamaterial absorber. *IEEE Photonics Journal*, *7*(1), pp.1-6.

[13] Wang, N., Tong, J., Zhou, W., Jiang, W., Li, J., Dong, X. and Hu, S., 2015. Novel quadruple-band microwave metamaterial absorber. *IEEE Photonics Journal*, *7*(1), pp.1-6.

[14] Engheta, N., 2003, June. Metamaterials with negative permittivity and permeability: background, salient features, and new trends. In *IEEE MTT-S International Microwave Symposium Digest, 2003* (Vol. 1, pp. 187-190). IEEE.

[15] Soukoulis, C.M., Kafesaki, M. and Economou, E.N., 2006. Negative-Index Materials: New Frontiers in Optics. *Advanced materials*, *18*(15), pp.1941-1952.

[16] Reed, E.J., Soljačić, M. and Joannopoulos, J.D., 2003. Reversed Doppler effect in photonic crystals. *Physical review letters*, *91*(13), p.133901.

[17] Pocklington, H.C., 1905. Growth of a Wave-group when the Group-velocity is Negative. *Nature*, *71*(1852).

[18] Rao, R., 2015. Microwave Engineering; PHI Learning Pvt. *Ltd.: Delhi, India*.

[19] Xu, W., Xie, L. and Ying, Y., 2017. Mechanisms and applications of terahertz metamaterial sensing: a review. *Nanoscale*, *9*(37), pp.13864-13878.

[20] Mallmann, E.J.J., Sombra, A.S.B., Goes, J.C. and Fechine, P.B.A., 2013. Yttrium iron garnet: properties and applications review. *Solid State Phenomena*, *202*, pp.65-96.

[21] Chlan, V., Štěpánková, H., Englich, J., Řezníček, R., Kouřil, K., Kučera, M. and Nitsch, K., 2010. Antisite Defects in Epitaxial Films of Lutetium Doped Yttrium Iron Garnets Studied by Nuclear Magnetic Resonance. *Acta Physica Polonica A*, *118*(5), pp.846-847.

[22] Khan, M.I., Waqas, M., Naeem, M.A., Hasan, M.S., Iqbal, M., Mahmood, A., Ramay, S.M., Al-Masry, W., Abubshait, S.A., Abubshait, H.A. and Mahmood, Q., 2020. Magnetic behavior of Ga doped yttrium iron garnet ferrite thin films deposited by sol-gel technique. *Ceramics International*, *46*(17), pp.27318-27325.

[23] Pozar, D.M., 2021. *Microwave engineering: theory and techniques*. John wiley & sons.

[24] Griffiths, D.J. and Colleger, R., 1999. Introduction to Electrodynamics Prentice Hall Upper Saddle River. *New Jersey*, *7458*.